

Experimental study on influencing factors of fracture propagation in fractured carbonate rocks

Yintong Guo^{a,*}, Longfei Hou^b, Yiming Yao^c, Luo Zuo^c, Zhiying Wu^c, Lei Wang^a

^a State Key Laboratory of Geomechanics and Geotechnical Engineering, Institute of Rock and Soil Mechanics, Chinese Academy of Sciences, Xiaohongshan, Wuchang, Wuhan, 430071, China

^b State Key Laboratory for Coal Mine Disaster Dynamics and Control, Chongqing University, Shazhengjie, Shapingba, Chongqing, 400044, China

^c State Key Laboratory of Shale Oil and Gas Enrichment Mechanisms and Effective Development, SINOPEC Research Institute of Petroleum Engineering, Beichen East Road, Beijing, 100101, China

ARTICLE INFO

Keywords:

Carbonate rocks
Gelled acid
Hydraulic fracturing
Fracture morphology characteristics
Composite fracturing
Fracturing fluid

ABSTRACT

Carbonate reservoirs show poor porosity and permeability in matrix, it is necessary to improve the permeability channel through reservoir reconstruction. The influence of different fracturing parameters on fracture propagation of carbonate rock is studied, which is of great significance to hydraulic fracturing design of carbonate rock. In this paper, a series of hydraulic fracturing experiments were performed under different conditions, the fracturing pump pressure curve, radial deformation characteristics and fracture morphology were studied and analyzed. The results show that: (1) The rock-acid reaction between gelled acid and carbonate rock produces etching wormholes, changes the pore structure and weakens the mechanical parameters of carbonate rocks, which is conducive to reducing fracturing pressure and increasing fracture complexity; (2) The types of fracturing fluids and the viscosity significantly affect fracturing rupture pressure and the width of the fracture. Under the same in-situ stress and flow rate conditions, the fracturing rupture pressure of slick water is the lowest and that of guar gum is the highest; (3) Composite fracturing can improve the complexity of fractures in carbonate reservoir, for carbonate rocks with fracture developed near wellbore, complex fracturing fractures can be made by slick water fracturing, and main fracturing surfaces can be eroded by gelled acid to improve the width and increase the roughness. (4) To solve the problem of high fracturing pressure under high in-situ stress, gelled acid can be used for pretreatment to reduce fracturing pressure, and then non-reactive fluid, slick water or guar gum can be used for fracturing. Our research findings provide a reliable basis for deep fractured carbonate reservoir reconstruction.

1. Introduction

Carbonate reservoir contain 52% of the world's total oil and gas reserves. The oil and gas production of carbonate reservoirs in the world accounts for about 60% of total oil and gas production (Jiang et al., 2008). At present, marine carbonate reservoir is one of the key and hot areas in oil and gas exploration and development (Wang et al., 2012). However, the permeability of carbonate matrix is usually less than 1 mD (Lucia, 2007). Generally, carbonate reservoirs need to be reformed to achieve commercial development. It is necessary to adopt hydraulic fracturing for reservoir reconstruction. The application of SRV technology to the development of carbonate rocks has important theoretical and practical significance.

In the process of carbonate reservoir reconstruction, the technologies adopted by various countries are basically similar, including acidizing, acid fracturing and sand fracturing, and stimulation methods derived from different purposes. For example, acid fracturing technology of pre-fluids, multi-stage injection acid fracturing technology and multi-stage injection & closure acidification technology, etc (Wang et al., 2012). Many studies have shown that geological discontinuities (Such as faults and natural fractures) play an important role in the formation of complex fracture networks (Jeffrey et al., 2009; Fisher and Warpinski, 2012). In order to fully understand the formation mechanism of complex fracture network in carbonate rocks, it is first necessary to clarify the main factors affecting the propagation of fracturing fractures.

Hydraulic fracturing experiment physical simulation is an important

* Corresponding author.

E-mail addresses: yguo@whrsm.ac.cn (Y. Guo), 172721894@qq.com (L. Hou), yaoym.sripe@sinopec.com (Y. Yao), zuoluoxingfeng@163.com (L. Zuo), 45825086@qq.com (Z. Wu), jack906@hotmail.com (L. Wang).

<https://doi.org/10.1016/j.jsg.2019.103955>

Received 9 October 2019; Received in revised form 4 December 2019; Accepted 4 December 2019

Available online 17 December 2019

0191-8141/© 2019 Elsevier Ltd. All rights reserved.

technical means to study fracture propagation mechanism, and it is easy to observe the geometric shape of hydraulic fracturing cracks. In order to study these problems, a lot of hydraulic fracturing simulation experiments have been carried out (Huang et al., 2011; Cheng et al., 2018; Hou et al., 2018; Liu et al., 2018). The influence of multiple factors on fracture propagation law of shale horizontal wells was studied, and the fracture morphology was observed by high-energy CT scanning. The results show that the effect of flow rate on fracture complexity is different in different intervals (Guo et al., 2014). Using acoustic emissions, hydraulic fracture propagation under different applied stresses are carried out. The location of acoustic emission agrees well with the visual expression at the intersection of cracks on the specimen. Sequential AE activity is episodic, and discretization means that the propagation of cracks is not a simple process (Yashwanth et al., 2013). The fracturing mechanism was studied by using acoustic emissions (Matsunaga et al., 1993). Research results show that the permeability and structure have great influence on initiation and extension propagation mechanism of hydraulic fracturing fracture.

A series of hydraulic fracturing tests were carried out on cylindrical sandstone specimens. The process of initiation, propagation and closure of fracturing fractures were studied, and the surface and internal structure of fractured specimens were observed by microscopy and X-ray CT scanner. The results show that the evolution of fracturing fracture's width plays a dominant role (He et al., 2017). The propagation characteristics of visible surface cracks, main cracks and main crack surfaces were observed and discussed. The results show that the induced fractures on the surface mainly extend along natural cracks, layers and interlayers, and there exists the intersection of beddings sand interlayers (Zhao et al., 2018). Hydraulic fracturing of unconsolidated rocks was carried out, and the mechanism of fracture initiation and propagation under different confining pressures with different injection fluids was studied. The results show that confining pressure and fluid rheology have great influence on the fracture behavior of compacted sand. Injection of viscous Newton fluid and cross-linked gel mainly produces percolation related to borehole expansion (Bohlooli and Pater, 2006).

A new analytical model is proposed to describe the bottom hole pressure behavior of acid fracturing stimulation wells in multi-layer fractured carbonate reservoirs. Inter-pore flow between fracture and matrix and cross flow between acid fracturing simulation and non-simulation zone were captured (Shi et al., 2019). In orders to study the influence of vugs on hydraulic fracture propagation, a series of hydraulic fracturing experiments were performed. The main influencing factors and typical fracturing curve characteristics are studied and analyzed (Liu et al., 2019). Three main vug-hydraulic fracture interaction modes were observed in the experiments. The hydraulic fracturing mechanism of fracture initiation and propagation in carbonate rock is studied. The effects of injection fracturing fluid, pump flow rate, fracturing pressure curve characteristics and fracture morphology are studied (Guo et al., 2018). However, due to rock-acid reaction in carbonate rocks, the fracture extension morphology of carbonate rocks is obviously different from other rock masses. It is difficult to obtain accurate pump pressure parameters and fracture morphology.

In this study, a series of hydraulic fracturing experiments were performed to investigate the fracture initiation and propagation in fractured carbonate cores. Various factors on hydraulic fracture initiation and propagation, including in-situ stress factors, fracturing fluid, injection rate were investigated for the fracture initiation and propagation. In particular, gelled acid fracturing has been carried out. Moreover, the composite fracturing for carbonate reservoirs is also studied and analyzed. The fracturing pressure curve, fracture morphology, radial deformation characteristics were evaluated under different conditions. Our research results can provide a reliable basis for optimizing hydraulic fracturing design in fractured carbonate reservoirs.

2. Experimental method and procedure

2.1. Sample preparation

Carbonate rock is mainly composed of sedimentary carbonate minerals (calcite, dolomite, etc.), carbonate rocks are mainly divided into three types: porous carbonate reservoirs, fractured carbonate reservoirs and fractured-porous carbonate reservoirs. The carbonate cores are taken from Southwest area in Akesu, northern margin of Tarim Basin, China. Outcrop core acquisition of carbonate block is shown in Fig. 1. It can be observed that the core is silver-gray carbonate rock with thicker layers and well-developed fractured blocks. The mineral composition was analyzed by Bruker AXS D8-Focus X-ray diffract meter. The mineral component content is listed in Table 1. As can be seen from Table 1, carbonate rocks contain three mineral components, of which calcite accounts for 91.49%, dolomite 6.25% and quartz 1.99%; it is characterized by "great content in carbonate, while few in quartz and impurities".

In this paper, the micro-structures of carbonate samples were observed by scanning electron microscopy (SEM). The magnification of the electron microscope is set to 100, 800 and 2000 times respectively. Microscopic pore structure scanning results are shown in Fig. 2.

According to the micro-structure characteristics obtained by scanning electron microscopy, it can be seen that there are sheet-like sedimentary structures in the minerals, calcite enrichment zones are arranged closely, calcareous cementation between mineral particles is well, and with a few micro-pore fissures. It may be due to incomplete crystallization or dissolution of calcite. The massive calcite layers are arranged in layers and form interlayer support with other minerals. Quartz and dolomite are filled in the pore of mineral particles in disorder and have certain laminated morphology. It can be seen that there are many kinds of space types, such as dilatation or filling residual cracks, dissolution voids, intergranular voids and micro-cracks. Calcite has irregular angular shape and smooth cross section, its particle size is about 100–200 μm ; Dolomite is approximate foliation and accompanied by a small amount of granular minerals with complete crystalline morphology. The particle size of dolomite is about 50–150 μm . A small amount of quartz is filled in the intergranular pore, showing a spherical granular shape with a particle size of 20–50 μm .

According to the technical requirements of experimental research, standard samples for rock mechanics and hydraulic fracturing tests are processed. According to ISRM suggested methods, cylindrical samples with diameter of 50 mm, height of 100 mm and surface parallelism of 0.03 mm were used for uniaxial and triaxial compression tests. The Brazilian splitting test uses a disc with diameter of 50 mm and height of 25 mm. The carbonate cores were taken to process into cylinder samples with 200 mm height and 100 mm diameter were used for hydraulic fracturing tests. A 12-mm-diameter hole was drilled in each sample to simulate the wellbore, and the depth of the hole is 115 mm. The simulated casing is made of high strength stainless steel with diameter of 6 mm and length of 90 mm, and grooves are left at the outer end of the pipe (Guo et al., 2018). We use epoxy resin to seal casing and borehole annulus. A 30 mm-long casing-free well is used as fracture section. Fig. 3 shows the design of the sample used in the hydraulic fracturing test.

2.2. Testing equipment

The rock mechanics tests were conducted on MTS 815.04 rock mechanics test system. The maximum axial loading is 4600 kN, and the confining pressure can reach to 140 MPa. The strain gauge was used to record the axial and radial strains during the test. Hydraulic fracturing tests were carried out on servo-controlled rock mechanic testing system with fracturing fluid pump injection system (Guo et al., 2018). As shown in Fig. 4. The testing system can apply axial loading is 0–2000 KN and confining pressure is 80 MPa. The technical parameters of the fracturing pump injection system are: The maximum flow rate is 10.0 mL/s and the

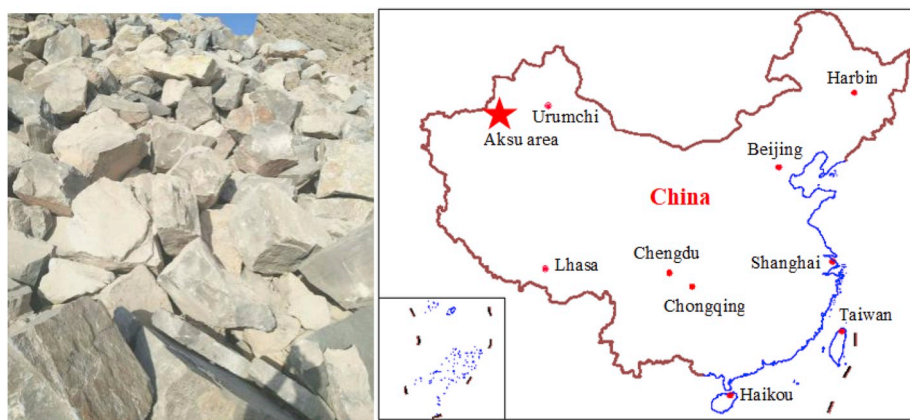


Fig. 1. Outcrop core acquisition of carbonate block.

Table 1

Calculation of mineral component content.

Sample No.	Mineral component content (%)		
	Calcite	Dolomite	Quartz
C-2	91.23	6.78	1.99
C-5	90.49	7.29	2.22
C-6	92.76	5.48	1.76
Average value	91.49	6.52	1.99

minimum flow rate is 0.01 mL/s. In addition, it can realize the conversion between different fracturing fluids.

2.3. Experimental methods

To investigate the effects of fracturing fluids and in-situ stress on hydraulic fracture propagation, the axial stress kept constant at 25 MPa in all experiments and confining pressures were 0 MPa, 10 MPa and 20 MPa, so different stress differences can be obtained. Three types of fracturing fluids are selected, slick water, guar gum and gelled acid. The viscosity of slick water is 3.5 mPa s the viscosity of guar gum is 230 mPa s and gelled acid is 80 mPa s. The flow rate is 0.07 ml/s. To visualize fracturing fractures caused by hydraulic fracturing and to better track

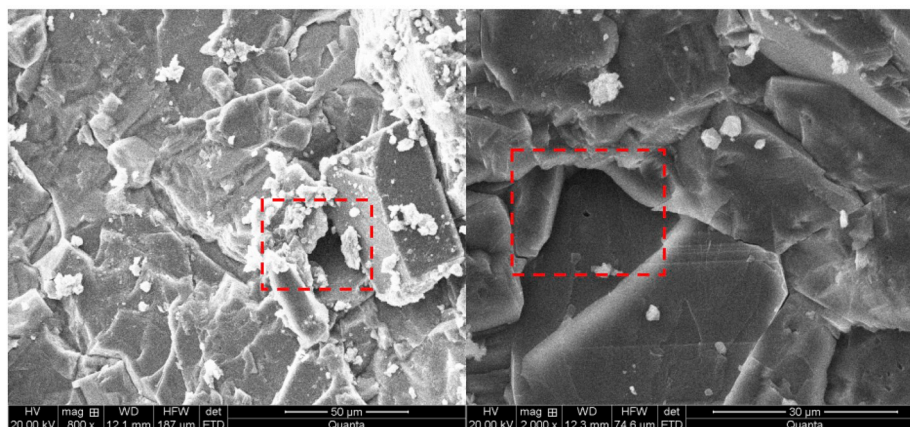
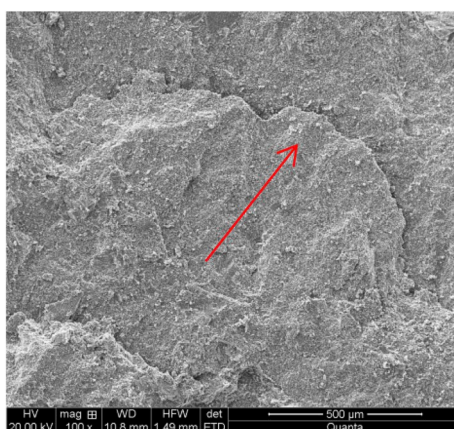


Fig. 2. Scanning micro-structure of carbonate rock by electron microscope.

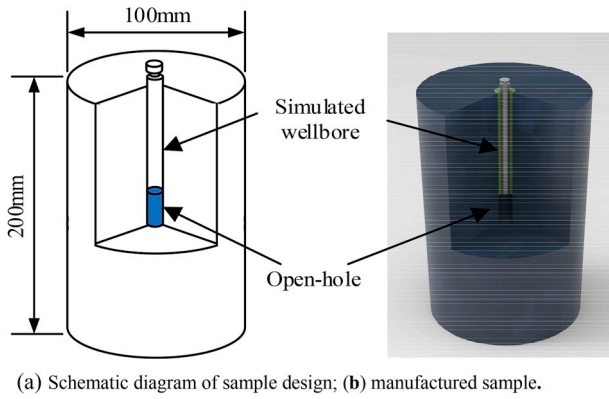


Fig. 3. shows the design of the sample used in the hydraulic fracturing test.

fracture morphology, red ink is added into the fracturing fluid. The experiment conditions are shown in Table 2.

A combination of non-reactive fracturing fluid (Slick water/guar gum) and reactive fracturing fluid (Gelled acid) are selected to form a composite fracturing mode, and two fracturing process schemes are formed.

Scheme 1: Firstly, hydraulic fracturing fracture is formed by direct fracturing with low flow rate slick water, and then acid-etched fracture is formed with gelled acid to increase fracture opening and fracture roughness.

Scheme 2: Firstly, 10 ml gelled acid was used to erode the core of the open hole section to degrade the physical and mechanical properties, After 10 ml of gelled acid is injected into the wellbore, the residual solution is extracted by syringe after the acid and rock react fully, and then hydraulic fracturing fracture was formed by fracturing with low flow rate slick water or guar gum. All the hydraulic fracturing test results were compared with the untreated samples.

Table 2

The results of hydraulic fracturing test.

Sample No.	Fracturing Fluid	Pump Flow Rate (mL/s)	σ_v (MPa)	$\sigma_H = \sigma_h$ (MPa)	Rupture Pressure (MPa)	Maximum radial deformation /mm
C-2-8	Slick water	0.07	25	0	11.03	1.440
C-3-2	Slick water	0.07	25	10	22.48	0.244
C-3-6	Slick water	0.07	25	20	31.69	0.162
C-2-4	Guar gum	0.07	25	0	12.19	4.624
C-3-8	Guar gum	0.07	25	10	26.66	0.820
C-3-2	Guar gum	0.07	25	20	41.82	0.487
C-0-8	Gelled acid	0.07	25	0	13.34	1.856
C-3-4	Gelled acid	0.07	25	10	26.19	0.331
C-3-9	Gelled acid	0.07	25	20	38.95	0.228

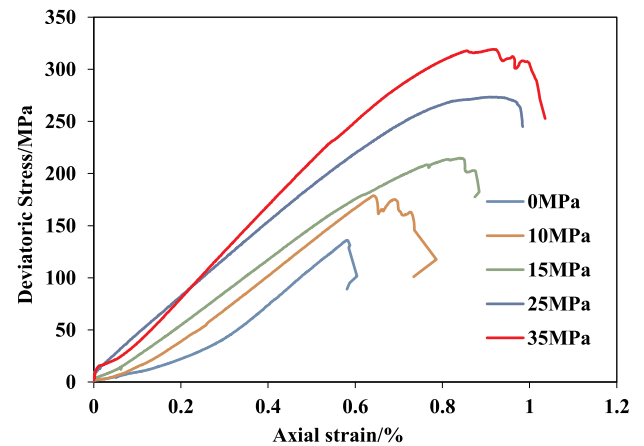


Fig. 5. Stress-strain curves under different confining pressures.



(a) Rock mechanical testing system. (b) Fracturing fluid pump injection system

Fig. 4. Hydraulic fracturing test system.

3. Experimental results and analysis

3.1. Rock mechanical properties

The mechanical properties of fractured carbonate rocks are important for determining the possibility of fracture initiation and propagation in materials. Fig. 5 is the stress-strain curves under different confining pressures. As can be seen from Fig. 5, with the increase of confining pressure, the peak deviatoric stress point of the curve corresponding to each specimen moves upward to the right, indicating that both the peak deviatoric stress and strain continue to increase, that is, the compressive strength and the amount of failure deformation increase. Under low confining pressure, the post-peak curve of sample has a certain slope. With the increase of confining pressure, the slope of the post-peak curve gradually slows down. It shows a tendency of brittleness under low confining pressure to ductility under high confining pressure. Moreover, it still has a certain bearing capacity after peak point, and the peak strength, residual strength and peak strain increase with the increase of confining pressure. Mechanical parameters of carbonate rocks under different confining pressures are listed in Table 3.

With the increase of confining pressure, when axial stress reaches the peak strength, the energy required for sample failure gradually increases. The elastic potential energy that can be released gradually decreases, and the dynamic failure phenomenon continues to weaken. The fracture mode is mainly shear failure, and with the increase of confining pressure, the number of fracture surfaces gradually decreases, the characteristics of brittle fracture gradually weaken, and the characteristics of ductile fracture gradually become obvious. Failure characteristics under different confining pressures are shown in Fig. 6. The failure mode is mainly tensile failure and shear failure, and the failure morphology has obvious characteristics of hard brittle rock failure. Failures under low confining pressure are characterized by the coexistence of cleavage and shear. With the increase of confining pressure, oblique shear slip failure mainly occurs in samples, the failure surface and failure angle change, and the failure surface becomes relatively smooth and even. In the process of failure, natural cracks existing in the sample may be destroyed.

Brazil splitting test were carried out on MTS 815.04. The axial displacement control mode was adopted; loading rate is 0.005 mm/s. The disc specimen is loaded in circular arc shape and loading by a constant displacement mode until the end of split test. The tensile strength is shown in Table 4. Fig. 7 is failure characteristics of Brazilian splitting test. It can be seen that the crack propagates along the direction of principal stress and then evolves from one principal crack into one or two secondary cracks. Along with the opening of the original crack, the specimen micro-crack expands rapidly and forms a macroscopic fracture surface in the direction of principal stress. There are secondary cracks on both sides of the main crack, and some secondary cracks are connected with the minor fracture surface. It provides conditions for the main fracturing fracture to communicate with natural fracture in hydraulic fracturing.

Table 3
Mechanical parameters of carbonate rocks under different confining pressures.

Sample No.	Confining pressures (MPa)	Deviatoric stress (MPa)	Peak axial strain (%)	Elastic Modulus (GPa)	Poisson's ratio
C-6-1	0	135.87	0.58	32.68	0.20
C-6-7	10	178.40	0.64	38.50	0.20
C-6-10	15	214.80	0.84	37.86	0.22
C-6-15	25	276.65	0.90	43.50	0.20
C-6-18	35	318.20	0.92	45.80	0.12

3.2. Micro-mechanism of gelled acid dissolution

The fracturing fluids used in fracturing of carbonate rocks are usually a combination of reactive and non-reactive fluids. The use of acid fluids can increase the complexity of rock micro-pore structure and degrade rock physical and mechanical properties during fracturing, and it can also influence fracture propagation during fracturing.

In order to study the effect of fracturing fluid on the degradation of mechanical properties of carbonate rocks, gelled acid was selected to carry out physical and mechanical properties tests after different erosion times under normal temperature and pressure conditions. The time is set to 30s, 2min, 5min, 30min and 120min. The changes of physical and mechanical properties of carbonate rocks before and after acid action are analyzed, and the average test results of each sample are shown in Table 5.

The acoustic velocity is a good index to reflect the comprehensive physical properties, which can reflect the mechanical properties of rock. As is shown in Fig. 8, the mass loss of carbonate samples and Vp velocity are obviously correlated with the increase of gelled acid soaking time. The loss rate and reduction rate are defined as the ratio of the difference between the average value of data at a certain time and the initial average value to the initial value, the mass loss rate and the Vp velocity decay rate were fitted. According to the scatter point and its fitting curve, the decrease of sample mass and Vp velocity can be divided into three processes: rapid decline, slow decline and tend to be gentle. Moreover, the degree and rate of decrease was the most obvious when soaked for 30min, and then almost stabilized though slightly changed.

To study the microstructure characteristics of carbonate rocks after gelled acid soaking, an electron microscope scanner was used. SEM scanning analysis was carried out after soaking for 0min, 0.5min, 2min, 5min, 30min and 120min, as shown in Fig. 9. Microstructure analysis shows that: in the initial state, the minerals present platy sedimentary structure, the calcite rich areas are arranged closely, the calcium cement between the mineral particles is good, and there are a few micro pore cracks. However, with the beginning of gelled acid erosion, the internal structure changes to different degrees, and it is most obvious that microscopic corrosion holes of different sizes are generated inside. The existence of corrosion holes will change the stress distribution in the core, and lead to local stress concentration, which will become the weak point. Meanwhile, the formation of corrosion holes will lead to reaction products and residual liquid entering the interior, thus degrading the mechanical strength characteristics. At the same time, the larger size of acid wormhole appeared in the structural surface of the mineral, and the unreacted acid around the acid wormhole would be lost along the wall of the acid wormhole, to change the internal structure. In the acid fracturing test, it was observed that the acid wormhole penetrated to the outer surface of the sample.

3.3. The influence of different fracturing factors

The primary pores in carbonate reservoirs are generally undeveloped with poor porosity and permeability, and low porosity and low permeability reservoirs are the majority with poor matrix permeability. Carbonate reservoirs need transformation to form certain productivity. Hydraulic fracturing and acidification fracturing are the main techniques of carbonate reservoir reconstruction. However, there are some technical problems in the transformation of carbonate rocks. The carbonate rocks are characterized by well-developed fractures, strong heterogeneity and serious acid leak-off, acidic rock reaction rate in high temperature reservoir is fast and non-uniform etching is insufficient, and fracture initiation and extension mechanism is complex, dynamic fracture width is small and sand adding is difficult. In this paper, research work has been carried out on the initiation pressure, fracture morphology and composite fracturing technology under different fracturing fluids.

Three types of fracturing fluids were selected for hydraulic fracturing

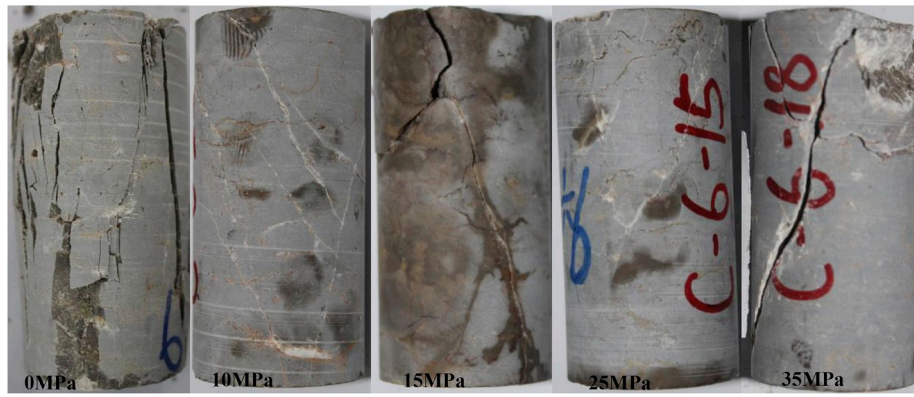


Fig. 6. Failure characteristics of carbonate samples under different confining pressures.

Table 4

Brazilian splitting test results of carbonate samples.

Sample No.	2	3	4	5
Maximum axial force F_n (kN)	14.61	16.28	14.51	15.03
Tensile strength σ_t (MPa)	7.81	8.69	7.80	8.05
Average tensile strength σ_t (MPa)	8.09			

tests. Two kinds of non-reactive fracturing fluids (Slick water & guar gum) and gelled acid fracturing fluids are used. The results of hydraulic fracturing test are listed in Table 2. The fracturing pump pressure curve, fracture morphology and radial deformation are obtained. Analysis of these factors is given in Sec. 3.3.1- 3.3.3, respectively.

3.3.1. Different fracturing fluids and different in-situ stress

Three kinds of fracturing fluids were used to conduct fracturing tests under three kinds of in-situ stress conditions. Fracturing pump pressure curves under different in-situ stress are shown in Fig. 10. According to Fig. 10, the characteristics of fracturing pressure curves obtained under different in-situ stresses are significantly different. In Fig. 10 (a), when the confining pressure is 0 MPa, in the initial stage of fracturing fluid injection, the fracturing pressure has a relatively slow growth stage. Because there is a small amount of air in the simulated wellbore, it is not excluded, and it has compressibility. With the injection of slick water, the fracturing pressure rises rapidly and drops rapidly after reaching breakdown pressure. The fracturing pressure continues to increase with injection fracturing fluid, which is lower than initial breakdown pressure, and multiple breakdown points are formed. When the confining pressure is 10 MPa, the fracturing pump pressure curve has only one peak point. When the peak pressure point is reached, the pressure drops rapidly to 12.31 MPa, and form stable fracturing fractures migration channels, with the continuous injection of slick water, the pump pressure will increase slightly. The pump pressure mainly overcomes confining pressure and frictional resistance of fracturing fracture. When

Table 5

Physical and mechanical parameters of carbonate rocks with different soaking time.

Sample No.	Soak time (min)	Quality loss rate (%)	Reduction rate of V_p (%)	Uniaxial compressive strength (MPa)	elasticity modulus (GPa)
1	0	0.00	0.00	151.5	35.92
2	0.5	0.05	1.09	128.8	31.98
3	2	0.13	2.08	107.6	26.74
4	5	0.29	3.33	102.0	26.06
5	30	2.01	6.19	91.0	19.14
6	120	2.42	6.25	87.4	19.29

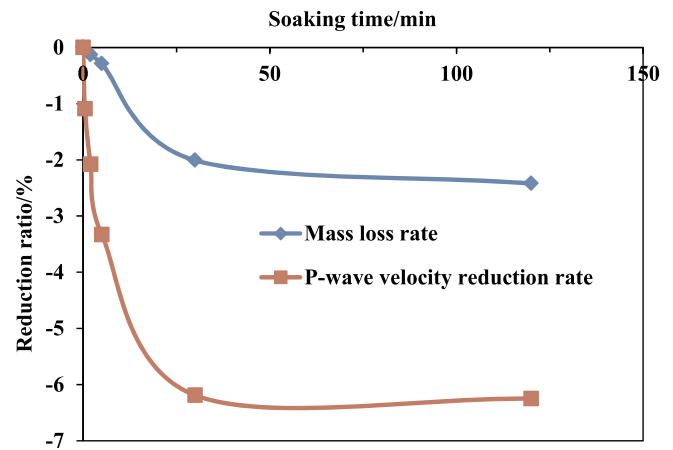


Fig. 8. The decay rate of petro physical parameters changes over time.



Fig. 7. Failure characteristics of Brazilian splitting test.

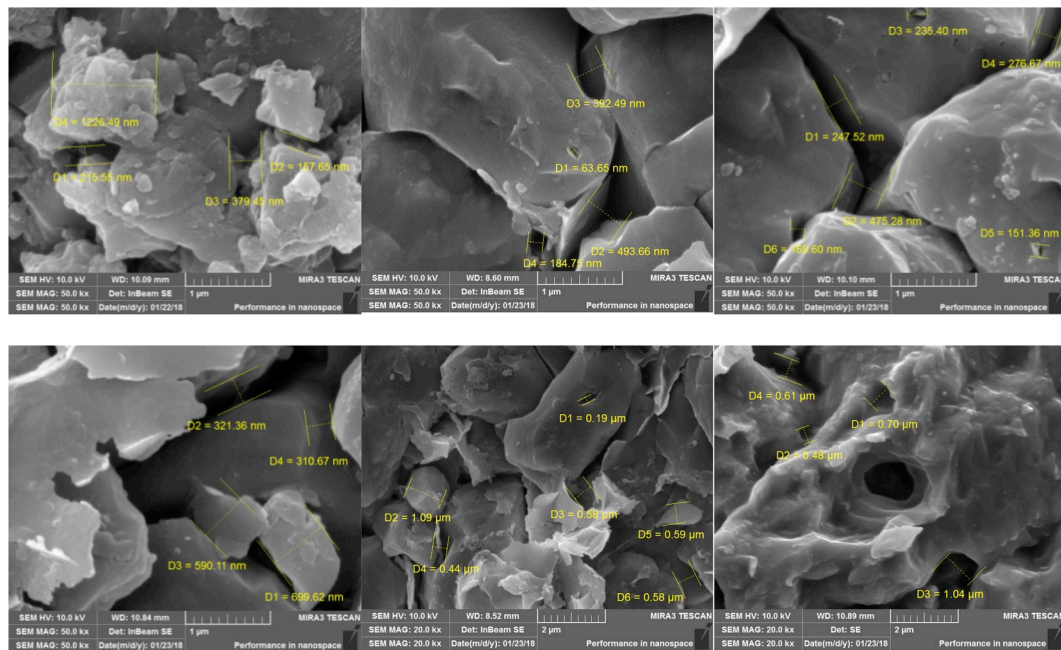


Fig. 9. Scanning electron microscopy microstructure characteristics.

confining pressure rises to 20 MPa, the fracturing breakdown pressure reaches 31.69 MPa, the curve characteristics are similar to those at confining pressure of 10 MPa. According to slick water fracturing under high in-situ stress conditions, the fracturing fracture morphology is relatively single.

When the guar gum with flow rate of 0.07 ml/s is used for fracturing, the characteristics of pump pressure curves are similar under three kinds of in-situ stress conditions, as shown in Fig. 10 (b). The fracturing pump pressure curve can be divided into three stages, first stage, the pump pressure increases slowly with the pumping of fracturing fluid; second stage, with the injection of fracturing fluid, the pump pressure increases rapidly, reaching the breakdown pressure point; third stage, after reaching breakdown point, when the fracturing fluid is pumped continuously, the pump pressure increases slowly and keeps relatively stable.

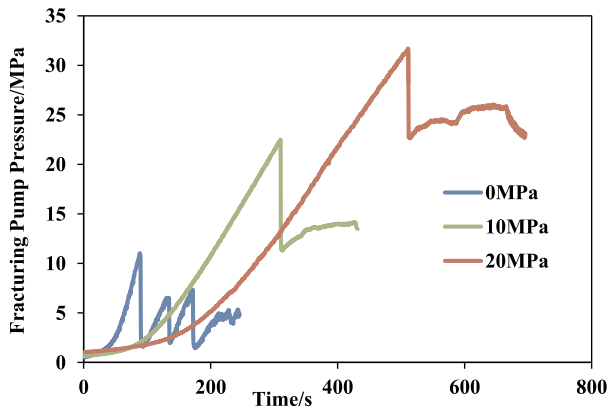
In order to understand the effect of acid fracturing fluid on fracture morphology of carbonate rock, gelled acid fracturing experiments were carried out. The viscosity of gel acid is 80 mPa s, and this kind of fracturing fluid is often used in carbonate reservoir. As can be seen in Fig. 10 (c), there are differences in fracturing pump pressure curve. When the confining pressure is 0 MPa, the gelled acid is injected into the sample, it has little effect on the mechanical properties of carbonate rocks in limited space and short time. When reaches the breakdown point, the fracturing pressure drops rapidly. The breakdown pressure usually indicates that a significant transverse main fracture has formed and the fracturing fluid continues to be pumped; fracturing pressure will be no longer increase. When the confining pressure increases, the fracturing pressure curve of gelled acid fracturing is similar to that of guar gum. During the fracturing test, the acid solution does not fully react with the rock, and the fracturing performance mainly depends on the viscosity of the fracturing fluid.

The deformation of sample under hydraulic fracturing can reflect the initiation and expansion of fracturing fracture. In order to analyze the initiation and scale information of fracturing fractures during fracturing fluid injection, the radial deformation of samples was collected simultaneously during hydraulic fracturing. Radial deformation in hydraulic fracturing under different in-situ stress is shown in Fig. 11. It can be seen from Figs. 10 and 11, for each fracturing pump pressure fluctuation point, radial deformation will also produce a fluctuation point; there is a

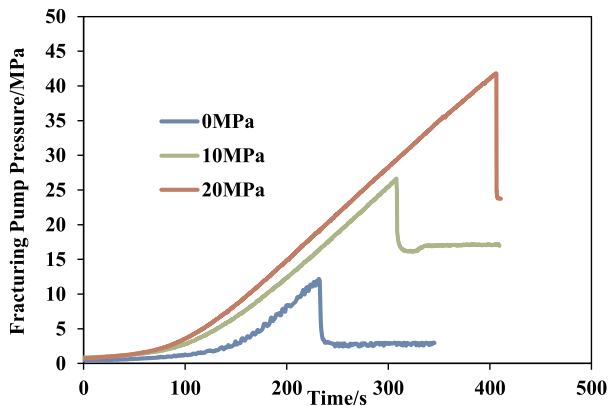
good correspondence between them. However, with the increase of confining pressure, the peak point of radial deformation decreases obviously. Fracturing with slick water, when the confining pressure is 0 MPa, the maximum radial deformation produced by fracturing is 1.440 mm; when the confining pressure increased to 20 MPa, the maximum radial deformation decreased to 0.162 mm. Fracturing with guar gum, when the confining pressure is 0 MPa, the maximum radial deformation produced by fracturing is 4.624 mm, at the same in-situ stress and flow rate, the maximum radial deformation produced by guar gum fracturing is the largest among the three fracturing fluids. When the confining pressure increased to 20 MPa, the maximum radial deformation decreased to 0.487 mm. The results show that the fracture width of hydraulic fracturing will decrease under high in-situ stress.

As can be seen in Fig. 12, the fracturing rupture pressure under different fracturing fluids is different. Under the same flow rate, the fracturing rupture pressure is the lowest when slick water is fracturing fluid. Low viscosity fracturing fluid is easy to pass through weak natural fractures or filling fractures, leading to micro-fracture opening and effectively reducing fracture pressure. When the confining pressure is 0 MPa, there is little difference in fracturing rupture pressure between the three fracturing fluids. The fracturing rupture pressure of slick water is 11.03 MPa, guar gum is 12.19 MPa, and gelled acid is 13.34 MPa. The maximum difference in absolute value is 2.31 MPa. However, when the confining pressure is 20 MPa, the fracturing rupture pressure of slick water is 31.69 MPa. The fracturing rupture pressure of guar gum is the highest, up to 41.82 MPa, the maximum difference in absolute value is 10.13 MPa. The research shows that for high in-situ stress in deep carbonate rocks, the initial fracturing with slick water can effectively reduce the initiation fracturing rupture pressure. Ensure the safety of fracturing equipment and increase the working depth.

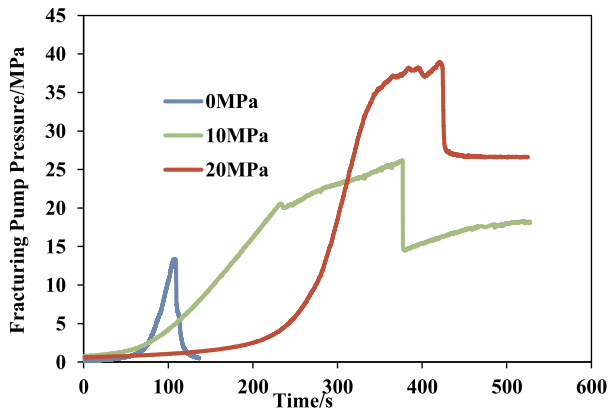
In the initial stage, gelled acid was used for direct fracturing, compared with guar gum fracturing; the decrease of fracturing rupture pressure is not obvious. When macroscopic fracture occurs during hydraulic fracturing, the radial deformation of the sample increases and changes suddenly. According to the change of radial strain, the deformation of fracturing fracture with fracturing pump pressure can be obtained. Fig. 13 is the comparison of maximum radial deformation under different fracturing fluids, it was shown that when confining pressure is 0 MPa, the fracturing rupture pressure of slick water fracturing is the



(a) Slick water

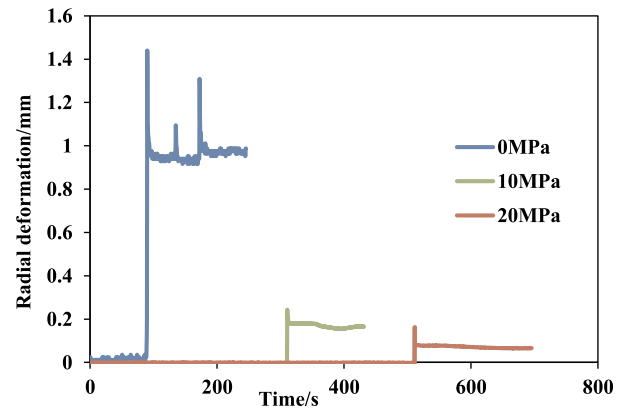


(b) Guar gum

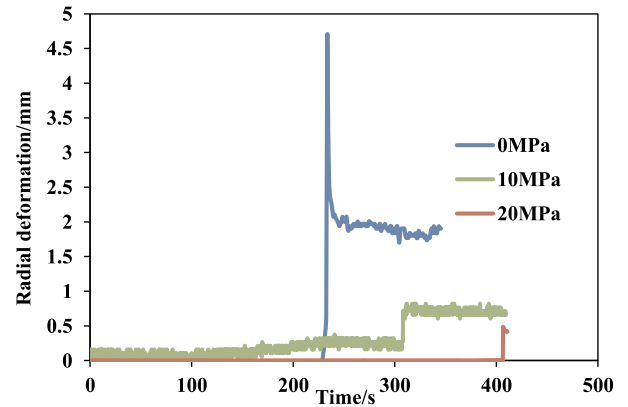


(c) Gelled acid

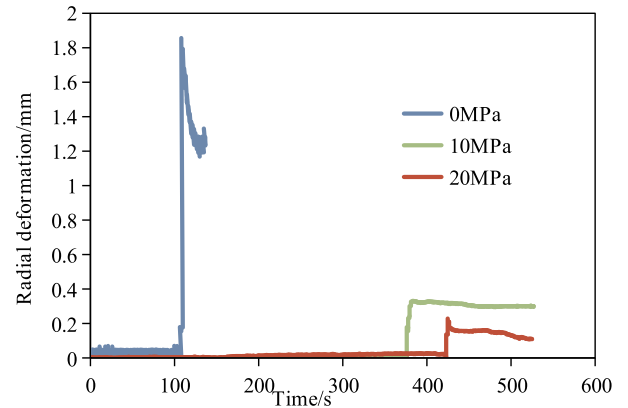
Fig. 10. Fracturing pump pressure curves under different in-situ stress.



(a) Slick water



(b) Guar gum



(c) Gelled acid

Fig. 11. Radial deformation in hydraulic fracturing under different in-situ stress.

lowest and that of guar gum fracturing is the highest. The radial deformation change of guar gum is 3.2 times that of slick water. The maximum radial deformation after gelled acid fracturing is 1.856 mm. The deformation difference between gelled acid and sliding water fracturing is small, and far less than guar gum. When gelled acid fracturing fluid is injected, rock-acid reaction will occur. According to the microstructure before and after acid action, acid wormholes will form inside the sample, resulting in smaller deformation during fracture. The results show that when high viscosity fracturing fluid is used, a transverse fracture has been formed and the fracture width is large.

Confining pressure has a significant effect on the initiation pressure, radial deformation and fracture morphology. With the increase of confining pressure, the fracturing ruptures pressure increases rapidly,

and the maximum radial deformation decreases. When confining pressure increases to 20 MPa, the maximum radial deformation of guar gum fracturing is 0.487 mm, compared with the confining pressure of 0 MPa, it decreases by 89.47%. And the radial deformation difference between guar gum fracturing and slick water fracturing is significantly reduced. The results show that under high in-situ stress, the width of fracturing fracture formed is mainly affected by in-situ stress, and the influence of fracturing fluid viscosity is gradually weakened.

3.3.2. Analysis of composite fracturing methods

In order to determine the influence of fracturing pump pressure and fracture morphology characteristics under the condition of composite

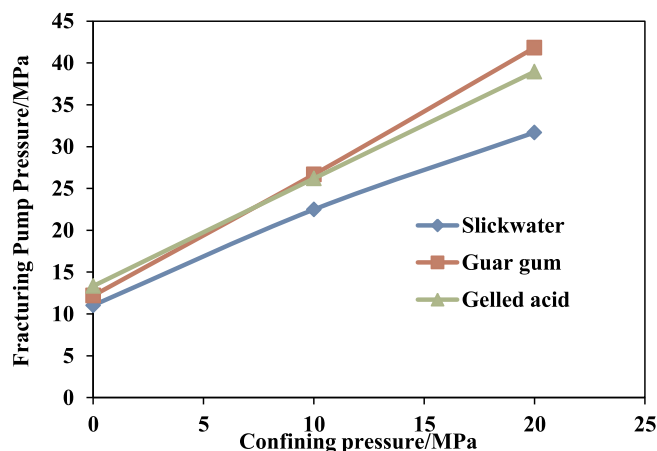


Fig. 12. Comparison of fracturing rupture pressure under different fracturing fluids.

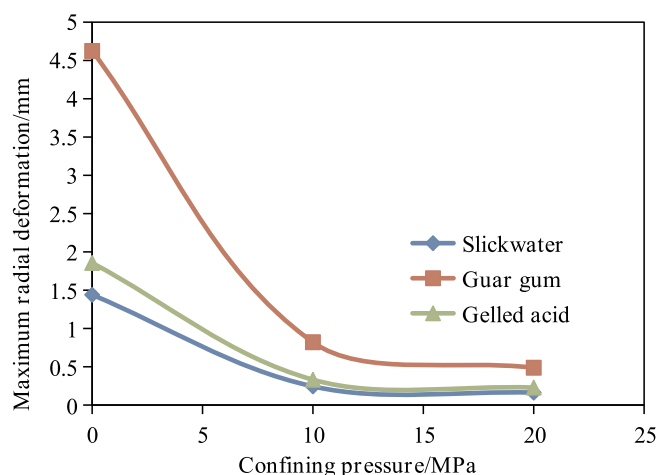
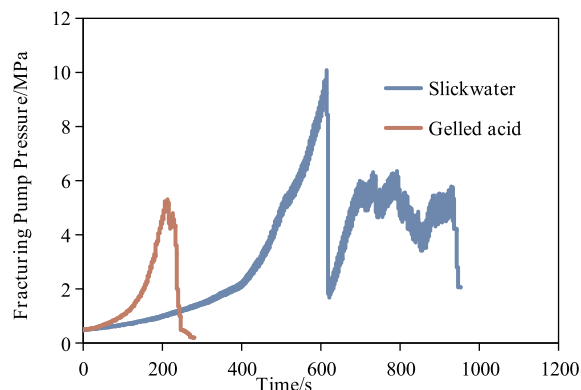
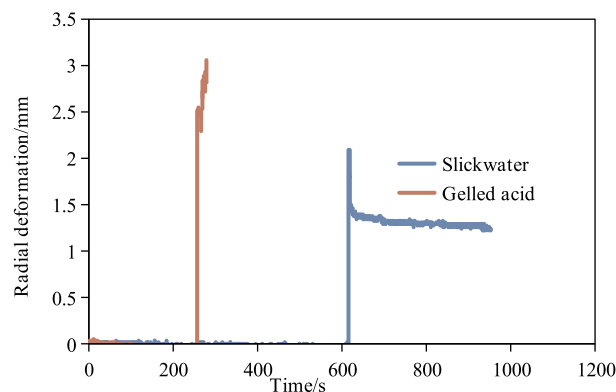


Fig. 13. Comparison of maximum radial deformation under different fracturing fluids.

fracturing with non-reactive fracturing fluid (Slick water and guar gum) and reactive fracturing fluid (Gelled acid), hydraulic fracturing tests were carried out under two combined conditions, Scheme 1: Firstly, hydraulic fracturing fracture is formed by direct fracturing with low-displacement slick water, when the pump pressure drops from one or more fracturing breakdown points to the extension pressure equivalent to the confining pressure, stop the pump system and switch to gelled acid. Then acid-etched fracture is fractured with high-displacement gelled acid to increase fracture opening and fracture network



(a) Fracturing pump pressure curve under composite fracturing



(b) Radial deformation curve under composite fracturing

Fig. 14. First fracturing by slick water with 0.02 ml/s, then fracturing by gelled acid with 0.02 ml/s.

roughness. Scheme 2: Firstly, the 10 ml gelled acid was used to erode the core of the open hole section to degrade the physical and mechanical properties, and then the hydraulic fracturing fracture was formed by direct pumping with low displacement slick water or guar gum. The results after composite fracturing test are shown in Table 6.

Fig. 14 is the fracturing pump pressure curve and radial deformation curve after composite fracturing. It can be seen from Fig. 14 (a), slick water fracturing fluid was injected, with a flow rate of 0.02 ml/s, and the fracturing pump pressure increased rapidly to 10.03 MPa and four peak pump pressures were generated. It indicates that natural cracks are opened inside the sample to form fractures with high complexity. Then, injection of gelled acid at a rate of 0.02 ml/s, the fracturing pump pressure increased to 7.16 MPa and then dropped rapidly to close to zero and no longer increased. It can be seen from Fig. 14 (b) that the radial deformation of the sample is still slightly larger than that of the slick

Table 6

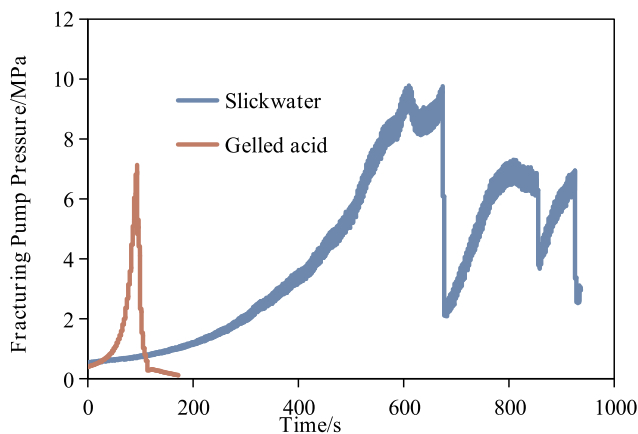
The results after composite fracturing test.

Sample No.	Fracturing Fluid	Pump Flow Rate (mL/s)	σ_v (MPa)	$\sigma_H = \sigma_h$ (MPa)	Rupture Pressure (MPa)	Maximum radial deformation /mm	Remarks information
C-1-5	Slick water	0.02	25	0	10.09	2.091	Fracturing by slick water
C-1-5-sy	Gelled acid	0.02	25	0	5.31	3.059	Fracturing of existing fractured specimens with gelled acid
C-1-6	Slick water	0.02	25	0	10.03	1.241	Fracturing by slick water
C-1-6-sy	Gelled acid	0.07	25	0	7.16	2.040	Fracturing of existing fractured specimens with gelled acid
C-2-1	Slick water	0.02	25	0	10.6	0.850	Fracturing by slick water
C-a-4	Slick water	0.02	25	0	8.07	2.308	Pretreatment with 10 mL gelled acid
C-2-3	Guar gum	0.02	25	0	10.3	4.590	Fracturing by guar gum
C-a-3	Guar gum	0.02	25	0	8.75	2.558	Pretreatment with 10 mL gelled acid

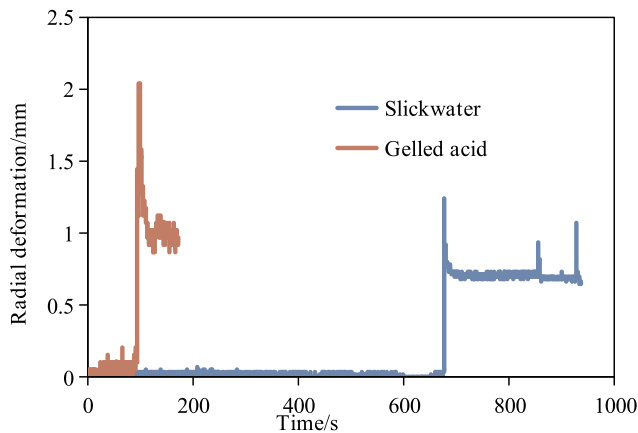
water when the gelled acid is continued to be pumped. This indicates that when fracturing with slick water, although a penetrating pressure fracture is formed, due to the small width of the fracturing fracture, when fracturing is continued with high viscosity gelled acid, the loss of fracturing fluid is less than the pumping amount, and fracturing pressure can still be restrained. The retention time of acid solution in fracture surface is increased, which is beneficial to acid rock reaction.

After fracturing with slick water, the gelled acid with different flow rate was used for further fracturing, and the fracturing pump pressure curve obtained was different. Fig. 15 is first fracturing by slick water with 0.02 ml/s, then gelled acid fracturing with 0.07 ml/s. It can be seen by comparing Table 2 and Fig. 15, when the pumping flow rate of gelled acid was increased to 0.07 ml/s, the corresponding fracturing peak pressure and maximum radial deformation were both increased when compared with flow rate of 0.02 ml/s, but the overall increase was small. It shows that the rate of injection of gelled acid has little effect on the fracturing pump pressure and radial deformation. The scheme has the effect of “reducing pump pressure, acid corrosion and fracture expansion”, the initiation fracturing pressure is obviously reduced, the width and length of fracturing fracture are increased and the fracture surface is rough.

10 ml gelled acid was injected uniformly for acid-etching pretreatment, and then slick water and guar gum were selected to carry out fracturing experiment. The fracturing test results are shown in Fig. 16 and Fig. 17. It can be shown that the fracturing pressure of the sample can be reduced after gelled acid treatment; the fracturing rupture pressure is reduced by 23.87% with slick water fracturing and reduced by 15.05% with guar gum fracturing. Moreover, the fracture point of

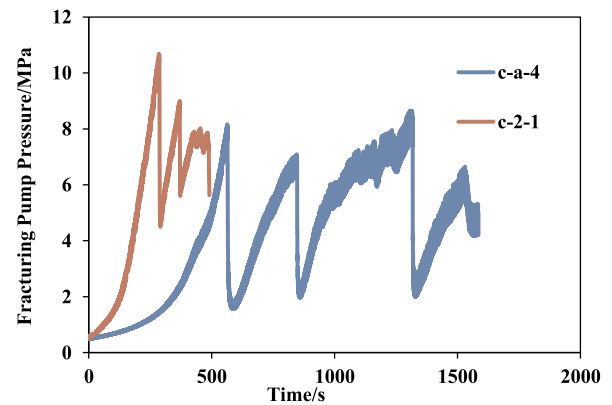


(a) Fracturing pump pressure curve under composite fracturing

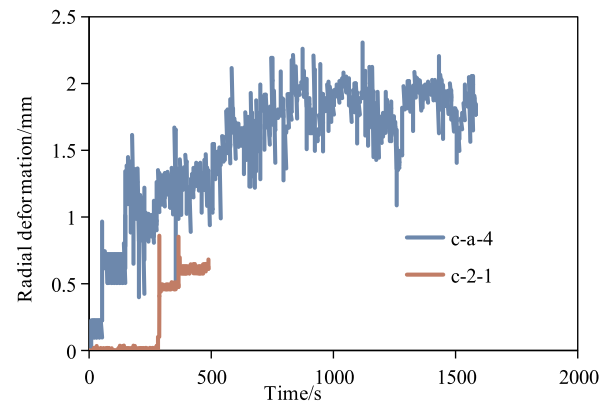


(b) Radial deformation curve under composite fracturing

Fig. 15. First fracturing by slick water with 0.02 ml/s, then fracturing by gelled acid with 0.07 ml/s.



(a) Fracturing pump pressure curve before and after gelled acid treatment



(b) Radial deformation curve before and after gelled acid treatment

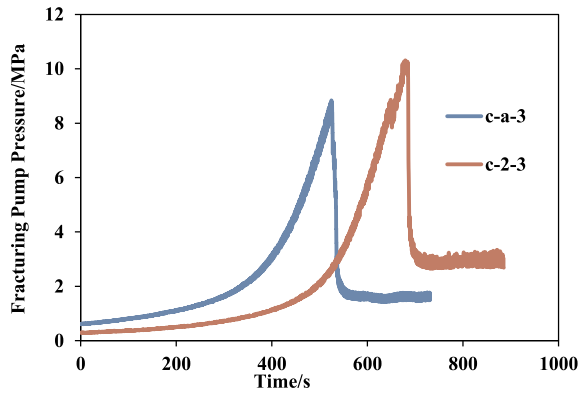
Fig. 16. Comparison of slick water fracturing characteristic before and after gelled acid treatment.

slick water fracturing has increased. After gelled acid treatment, the fractured section of the wellbore becomes irregular shape, and the radial deformation after fracturing generates violent fluctuations, which also proves that the pretreatment increases the complexity of the near-wellbore and is conducive to the generation of multiple fractures. These show that gelled acid can enter the open hole section of wellbore precast corrosion near wellbore attachment calcium minerals and form lots of secondary pores and micro-cracks, so as to enhance the capacity, core permeability and liquid absorption of the cracks in the process of fracturing fluid filtration, more easily lead to fracturing rupture pressure is reduced, at the same time, through principal compressive fracture, fracturing fluid is more likely to enter for porosity derived from secondary cracks, so as to increase the quantity type and cracks, form a complex network.

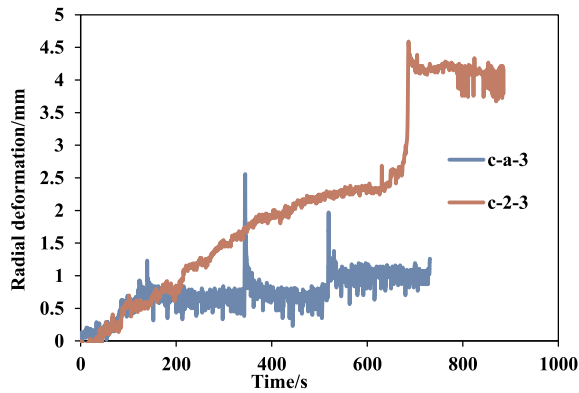
3.3.3. Fracture morphology characteristics

The fracture morphology of carbonate rocks after direct fracturing with slick water and guar gum is shown in Fig. 18. It can be seen from Fig. 18 (a), when slick water is used as fracturing fluid, multiple fractures intersecting the main fracturing fracture are observed on the surface and inside of the sample, creating more flow channels. After fracturing with guar gum, only a main fracturing fracture with certain bending was formed.

Fig. 19 is fracture morphology after composite fracturing. According to Fig. 19 (a) & (b), after fracturing with the combination of slick water and gelled acid, corrosion worm holes with a width of about 1 mm along the primary fracturing fracture can be seen on the surrounding surface of the samples. After gelled acid injection, the crack fracture growth mainly concentrated near the initial crack initiation. This indicates that when relatively complex fractures are formed by slick water fracturing;



(a) Fracturing pump pressure curve before and after gelled acid treatment



(b) Radial deformation curve before and after gelled acid treatment

Fig. 17. Comparison of guar gum fracturing characteristic before and after gelled acid treatment.

continue pumping gelled acid, the gelled acid preferentially enters the main pressure fractures near the wellbore, but not all the pressed fractures. The characteristics of fracturing fractures on the surface of samples after gelled acid etching treatment are shown in Fig. 19(c) and (d). After slick water fracturing, a main fracturing fracture is formed along the direction of maximum principal stress, and fracturing fluid diffuses along the fracture. Several secondary cracks intersecting the main crack were observed on the surface of the sample, and more flow channels were generated. When guar gum was used as fracturing fluid, only one major fracturing fracture was observed on the surface, due to the influence of natural cracks inside the sample, the deflection occurs in the middle of the sample.

It is difficult to obtain clear fracture morphology by direct observation. Combined with the results of high energy CT scan, the fracture morphology characteristics of with slick water fracturing without acid treatment and composite fracturing specimens were analyzed respectively. Fracture morphology after fracturing with slick water without acid treatment is shown in Fig. 20. It is found that the main crack is formed along the direction of the maximum principal stress, and opens

the natural weak surface in the direction of non-principal stress. The width of the fracturing fracture formed is very narrow, generally less than 0.2 mm. Fracture morphology after composite fracturing (Slick water + gelled acid) is shown in Fig. 21. As can be seen from Fig. 21, when using a composite fracturing of slick water and gelled acid, due to the large fracture and corrosion, the fracture interface is very obvious. A fracturing fracture with a width greater than 1.5 mm was formed on one side of the sample. The results show that the dissolution of gelled acid solution can increase the width of fractured fracture and improve the conductivity of carbonate reservoir.

4. Discussion

For fractured deep carbonate reservoirs, hydraulic fracturing alone is not enough to open natural fractures. Therefore, it is necessary to explore the fracture propagation pattern of fractured reservoirs. In this paper, the fracture morphology and fracturing rupture pressure under different conditions are studied. The non-reactive fracturing fluid and gelled acid fluid were used in the fracturing process. Due to the strong heterogeneity of fractured carbonate reservoirs, the properties of different strata vary greatly. Different fracturing technologies were selected according to the characteristics of carbonate reservoir. For carbonate reservoirs with relatively developed natural fractures; firstly, hydraulic fracturing can be conducted with low flow rate slick water, which can effectively activate the original natural fractures and form a complex fracture network. Then pump gelled acid with a certain flow rate, and the high conductivity of main fracture areas formed by gelled acid etching near the well zone. For deep carbonate reservoirs, when fractures do not develop near the wellbore, gelled acid pretreatment can be used to reduce the fracturing rupture pressure under the condition of high in-situ stress. On the one hand, the mechanical parameters of carbonate rock will be reduced. On the other hand, it can form micro-cracks in the wellbore wall. Then, hydraulic fracturing was carried out with low flow rate slicker water to facilitate a relatively complex fracture network. The technique is used to improve the effect of reservoir reconstruction.

5. Conclusions

Triaxial hydraulic fracturing simulation experiments for fractured carbonate were conducted. Three types of fracturing fluids were selected for hydraulic fracturing tests under in-situ stress. The fracture morphology and fracturing pump pressure curve characteristics under different conditions are obtained, and the characteristics under composite fracturing are compared and analyzed. The main conclusions are as follows.

- (1) The acid rock reaction between gelled acid and carbonate rocks easily produces acid-eroded wormholes, change the pore structure and weaken the mechanics parameters of carbonate rock, which is helpful to reduce the fracturing rupture pressure and increase the fracture complexity.
- (2) When the confining pressure is low, fracturing with slick water can produce multi-fracturing fracture characteristics. Under the

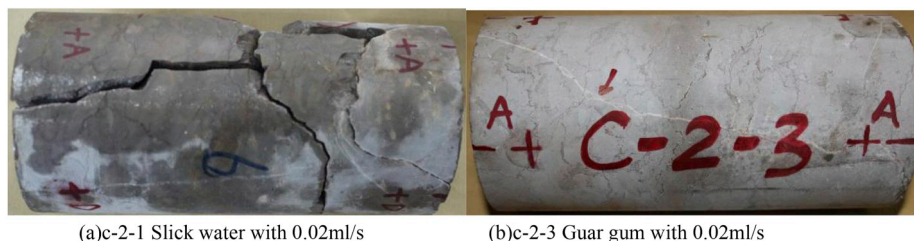


Fig. 18. Fracture morphology after direct fracturing.

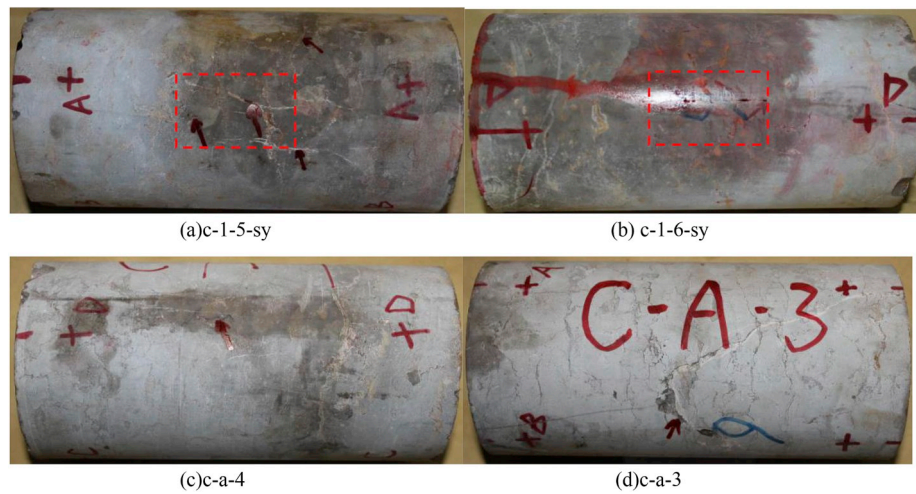


Fig. 19. Fracture morphology after composite fracturing.

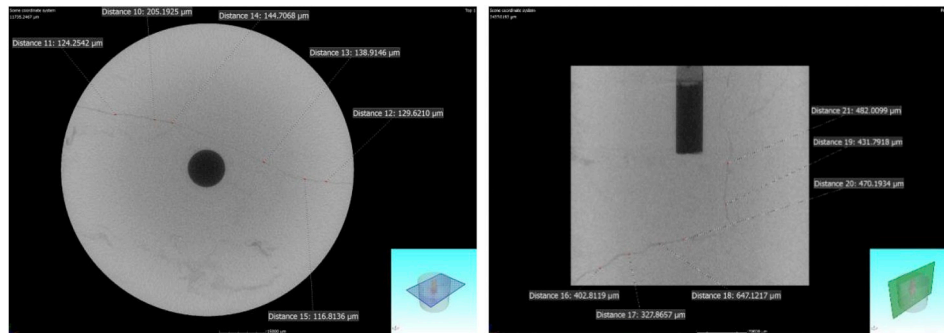


Fig. 20. Fracture morphology after fracturing with slick water without acid treatment.

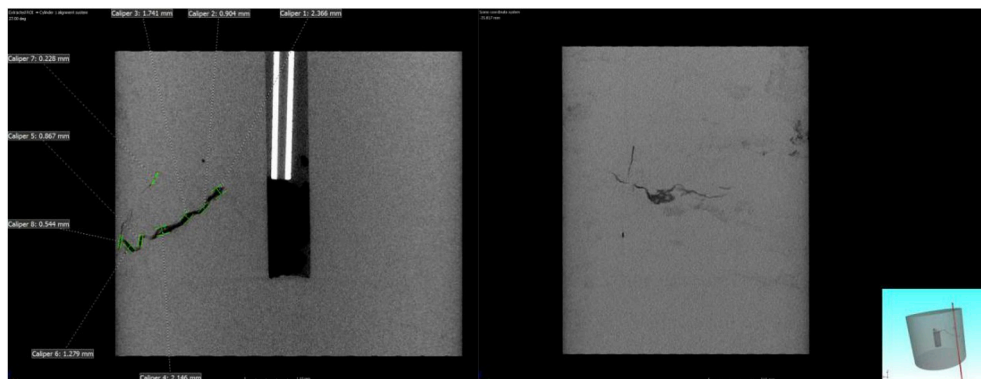


Fig. 21. CT scans of fracture morphology after composite fracturing (Slick water + gelled acid).

same in-situ stress and flow rate conditions, the fracturing rupture pressure of slick water is the lowest, and the guar gum is the highest, which is mainly affected by the viscosity of the fracturing fluid. Gelled acid fracturing has limited acid rock reaction in a short time, and does not significantly reduce fracturing rupture pressure, and the fracture after fracturing is mainly acid-etched wormholes.

- (3) Confining pressure has a significant effect on the initiation pressure, radial deformation and fracture morphology. With the increase of confining pressure, the fracturing ruptures pressure increases rapidly, and the width of fracturing fracture decreases significantly.

- (4) For fractured carbonate rocks, firstly, slick water fracturing can be used to activate more natural fractures, and then gelled acid is used to etch with existing fractured fractures, which can effectively improve the fracture width and increase the roughness, it is conducive to the formation of oil and gas permeability channels.
- (5) For the problem of high fracturing pressure under high in-situ stress, gelled acid can be used for pretreatment to reduce the fracturing pressure, and then non-reactive liquid, slick water or guar gum can be used for fracturing.

Funding

The research was supported by National Natural Science Foundation of China (51574218), National Science and Technology Major Project of China (2017ZX05005-004, 2017ZX05036-003) and Sinopec Ten Dragons Project (P18058). We would like to express our greatest gratitude for their generous support.

Data availability

The [DATA TYPE] data used to support the findings of this study are available from the corresponding author upon request.

Declaration of competing interest

The authors declare no conflict of interest.

CRediT authorship contribution statement

Yintong Guo: Conceptualization, Writing - original draft. **Longfei Hou:** Data curation. **Yiming Yao:** Formal analysis. **Luo Zuo:** Investigation. **Zhiying Wu:** Methodology. **Lei Wang:** Writing - review & editing.

References

- Bohlooli, B., Pater, C.J., 2006. Experimental study on hydraulic fracturing of soft rocks: influence of fluid rheology and confining stress. *J. Pet. Sci. Eng.* 53, 1–12.
- Cheng, Y.G., Lu, Y.Y., Ge, Z.L., Cheng, L., 2018. Experimental study on crack propagation control and mechanism analysis of directional hydraulic fracturing. *Fuel* 218, 316–324.
- Fisher, M.K., Warpinski, N.R., 2012. Hydraulic-fracture-height growth: real data. *SPE Prod. Oper.* 27 (1), 8–19. SPE-145949-PA.
- Guo, T.K., Zhang, S.C., Qu, Z.Q., et al., 2014. Experimental study of hydraulic fracturing for shale by stimulated reservoir volume. *Fuel* 128, 373–380.
- Guo, Y.T., Deng, P., Yang, C.H., et al., 2018. Experimental investigation on hydraulic fracture propagation of carbonate rocks under different fracturing fluids. *Energies*.
- He, J.M., Lin, C., Li, X., et al., 2017. Initiation, propagation, closure and morphology of hydraulic fractures in sandstone cores. *Fuel* 208, 65–70.
- Hou, B., Zhang, R.X., Zeng, Y.J., et al., 2018. Analysis of hydraulic fracture initiation and propagation in deep shale formation with high horizontal stress difference. *J. Pet. Sci. Eng.* 170, 231–243.
- Huang, B.X., Liu, C.Y., Fu, J.H., 2011. Hydraulic fracturing after water pressure control blasting for increased fracturing. *Int. J. Rock Mech. Min. Sci.* 48, 976–983.
- Jeffrey, R.G., Bunger, A.P., Lecampion, B., et al., 2009. Measuring hydraulic fracture growth in naturally fractured rock. In: Presented at the SPE Annual Technical Conference and Exhibition, New Orleans, Louisiana, USA, SPE-124919-MS.
- Jiang, H.Y., Song, X.M., Wang, Y.J., et al., 2008. Current situation and forecast of the world's carbonate oil and gas exploration and development. *Offshore Oil* 28 (4), 6–13.
- Liu, J., Yao, Y.B., Liu, D.M., et al., 2018. Experimental simulation of the hydraulic fracture propagation in an anthracite coal reservoir in the southern Qinshui basin, China. *J. Pet. Sci. Eng.* 168, 400–408.
- Liu, B.H., Jin, Y., Chen, M., 2019. Influence of vugs in fractured-vuggy carbonate reservoirs on hydraulic fracture propagation based on laboratory experiments. *J. Struct. Geol.* 124, 143–150.
- Lucia, F.J., 2007. *Carbonate Reservoir Characterization*, 2th ed. Springer Berlin Heidelberg.
- Matsunaga, I., Kobayashit, H., Sasaki, S., Ishida, T., 1993. Studying hydraulic fracturing mechanism by laboratory experiments with acoustic emission monitoring. *Int. J. Rock Mech. Min. Sci. Geomech. Abstr.* 30 (7), 909–912.
- Shi, W., Yao, Y., Cheng, S., Shi, Z., 2019. Pressure transient analysis of acid fracturing stimulated well in multilayered fractured carbonate reservoirs: a field case in Western Sichuan Basin, China. *J. Pet. Sci. Eng.* <https://doi.org/10.1016/j.petrol.2019.106462>.
- Wang, Y.H., Li, Y.P., Cheng, X.S., et al., 2012. A new acid fracturing technique for carbonate reservoirs with high-temperature and deep layer. *Acta Pet. Sin.* 33 (2), 166–173.
- Yashwanth, C., Camilo, M., Carl, S., Chandra, R., 2013. An experimental investigation into hydraulic fracture propagation under different applied stresses in tight sands using acoustic emissions. *J. Pet. Sci. Eng.* 108, 151–161.
- Zhao, Z.H., Li, X., He, J.M., et al., 2018. Investigation of fracture propagation characteristics caused by hydraulic fracturing in naturally fractured continental shale. *J. Nat. Gas Sci. Eng.* 53, 276–283.